Analyzing Earth's Position based on the Anisotropic Characteristics of Cosmic Microwave Background Radiation

Muhammad Khaidir Komala, Ahmad Aminuddin Bama* & Supardi
Physics Study Program, University of Sriwijaya, Indonesia
*Corresponding author: akhmad_aminuddin_bama@mipa.unsri.ac.id

Received: 30 November 2023; **Accepted**: 18 December 2023; **Published**: 20 December 2023
DOI: https://dx.doi.org/10.29303/jpft.v9i2.6284

Abstract - *This paper elaborates on the results of an exhaustive study regarding the Earth's position in the universe based on the Cosmic Microwave Background (CMB) radiation map, which is the latest discovery in modern astronomy. CMB radiation provides crucial insights into the early distribution of mass and energy in the universe. The aim of this research is to understand the theory and mechanisms behind the formation of polarity structures in the CMB and analyze their correlation with Earth's position in the overall structure of the universe. Intensity measurement data of CMB radiation published by COBE, WMAP, and Planck present temperature distribution data in coordinates in FITS (Flexible Image Transport System) format files. Subsequently, a spherical harmonic transformation is performed to obtain spherical harmonic coefficients a_lm as equations that represent dipole, quadrupole, octupole models, and various other multipole models. The analysis of the correlation in the temperature distribution of CMB radiation involves detailing various patterns found in the dipole, quadrupole, and octopole models, demonstrating quasi-symmetry characteristics with Earth at its center. An analysis of anisotropic CMB data yields an interesting hypothesis that the Earth's position plays a role in shaping the structure of the universe on a certain scale. Even more extremely, it can be said that Earth is at the center of the universe. This finding prompts profound contemplation about Earth's position in the structure of the cosmos, opening the door for further research in this field.*

Keywords: *Cosmic Microwave Background Radiation; Spherical Harmonic; Dipole.*

INTRODUCTION

Since Nicolaus Copernicus proposed the Heliocentric model in the 16th century, the belief in the non-central position of Earth has deeply rooted. However, recent data in modern astronomy, especially from the map of cosmic microwave background radiation (CMBR), presents a new paradox regarding Earth's position in the universe. Intriguing findings from the CMB, such as harmonic spherical structures encompassing dipole, quadrupole, and octopole, raise profound questions about the alignment of Earth's position with the observed cosmological structures.

The discovery of Cosmic Microwave Background (CMB) radiation by Penzias and Wilson in 1964 marked a crucial milestone in understanding the universe. This radiation, originating from the early moments of the universe, provides vital clues about the distribution of mass and energy (Penzias and Wilson, 1965). Anisotropic CMB data reveals alignment patterns between Earth's position and cosmological structures, leading to the hypothesis that Earth's position may play a role in shaping the universe's structure on a certain scale (Land and Magueijo, 2007). Therefore, this research aims to comprehend the theory and mechanisms behind the formation of polarity structures in the CMB and analyze the correlation between CMB polarity structures and Earth's position in the cosmic structure. It is expected that this study will offer new insights into the unique role and influence of Earth in the broader cosmological context.

Cosmic Microwave Background Radiation (CMBR)

Cosmic Microwave Background Radiation (CMBR) is the electromagnetic radiation that pervades the entire universe. It was serendipitously discovered by Penzias and Wilson while measuring zenith noise at the Crawford Hill Laboratory in Holmdel, New Jersey. They observed an excess noise of about 3,5° K that couldn't be explained, later confirmed to be the CMBR (Penzias and Wilson, 1965). Subsequently, Dicke explained that the anomaly in the noise measurement was evidence of the presence of cosmic blackbody radiation predicted and attempted to explain for the past two decades (Dicke et al., 1965). Earlier, in 1948, Alpher and Herman had theoretically predicted the possibility of blackbody radiation with a temperature of approximately 5° K flooding the universe from the primordial cosmos (Alpher and Herman, 1948). However, the temperature calculations of its noise were not accurate, and there was no strong supporting evidence until it was accidentally discovered by Penzias and Wilson

In its early discovery, microwave radiation was highly controversial as it became a battleground for proponents of the steady-state universe and the Big Bang universe. Wickramasinghe and Narlikar were convinced that microwave radiation did not deviate from the steady-state universe theory. They relied on previous research indicating that the radiation originated from the scattering of light from distant stars, as the thermal spectrum of blackbody radiation in microwaves resembled the energy produced by the conversion of hydrogen into helium in all galaxies (Wickramasinghe and Narlikar, 1967). In the 1970s, the consensus increasingly shifted away from the relevance of the steady-state universe theory. Various studies, including light elements in the universe, large-scale structure, cosmic inflation, and the discovery of cosmic microwave background radiation, supported a model of the universe more in line with the Big Bang theory. This perspective was further strengthened by research results published by COBE (Peebles et al., 1991).

Measurement of CMB Radiation Noise Temperature

Holmdel Horn Antenna is a large microwave horn antenna located at the Crawford Hill Laboratory in Holmdel, New Jersey. The antenna functions to receive and transmit electromagnetic wave signals in various frequency ranges, including microwaves and radio waves (Crawford, Hogg, and Hunt, 1961). In their research, Penzias and Wilson measured the sensitivity of the Holmdel Horn Antenna at a frequency of 4080 Mc/s (or MHz) or 4.08 GHz (Penzias and Wilson, 1965). Antenna sensitivity is a crucial parameter that describes how well an antenna can detect and respond to weak signals. Antenna sensitivity is measured by connecting it to a reference signal source with known intensity and characteristics, typically with a stable temperature. The measured antenna is then connected to the signal source via coaxial cables or appropriate connecting systems. The resulting output includes the reference signal and additional noise received by the antenna. Subsequently, the noise is measured using sensitive equipment such as a spectrum analyzer to obtain the Noise Figure (NF) or Noise Temperature (Tn). The Noise Figure indicates how much additional noise the antenna captures compared to the reference signal, while the Noise Temperature describes the effective temperature of that noise (Crawford, Hogg, and Hunt, 1961). From the measured noise at a frequency of 4080 MHz, the total measured noise temperature was 6.7° K. This noise temperature consists of 2.3° K contributed by atmospheric absorption and 0.9° K contributed by resistance losses. Therefore, among the various factors causing this noise, the remaining temperature of 3.5° K was identified as the Cosmic Microwave Background Radiation (Penzias and Wilson, 1965).

The antenna's sensitivity can be represented in the form of noise temperature (Tn) because microwave signals are electromagnetic waves with a relationship that is inversely proportional to temperature. According to Wien's displacement law, the peak wavelength ($\lambda_{\max}$) of the radiation spectrum emitted by a black body is inversely proportional to its absolute temperature (T) expressed by the formula:

$$\lambda_{\max} = \frac{C}{T} \quad (1)$$

where C is the Wien displacement constant (2,897771955 x 10^{-3}^ mK) (Aprilia et al., 2022; Ball, 2013; Das, 2015; Williams, 2014).

The relationship between temperature and electromagnetic waves is further explained through Planck's radiation law, which states that the intensity of the electromagnetic radiation spectrum $I(\lambda)$ emitted by a black body at a specific temperature (T) depends on the wavelength, given by the formula:

$$I(\lambda) = \frac{2hc^2}{\lambda^5} \frac{1}{e^{\frac{hk}{\lambda kT}} - 1} \quad (2)$$

where h is the Planck constant (6,62607015 x 10^{-34} J·s), λ is the wavelength of the radiation, and k is the Boltzmann constant (1,380649 x 10^{-23} J/K) (Derlet and Choy, 1996; Planck, 1914).

Cosmological Principle

When studying cosmology, there are two cosmological principles that need to be considered, namely isotropy and homogeneity. Isotropy means that the universe appears the same from all directions, indicating that the properties of the universe do not depend on the direction of observation. On the other hand, homogeneity means that the universe has a similar structure on very large scales. This implies that when observing the sky with a telescope and examining the distribution of galaxies, the distribution should be relatively uniform in all directions and locations in the sky (Abramo and Pereira, 2010; Andrade et al., 2018; Clarkson and Maartens, 2010; Goodman, 1995; Peebles, 1993; Weinberg, 2008; Zhou et al., 2017). However, in reality, the universe is not entirely isotropic and homogeneous; there are observed irregularities or inconsistencies, known as anisotropies.

Anisotropy in CMB Radiation

Anisotropy in cosmic background radiation (CMB) refers to small variations in the temperature of radiation from one direction to another. Anisotropy can also be found in the large-scale structure of the universe, such as galaxies and galaxy clusters, providing clues about the evolution of the universe and the nature of matter and energy within it. Anisotropy in CMB consists of two types: primary and secondary. Primary anisotropy occurs when cosmic sound waves propagate through matter during the radiation era. When these waves reach the point where matter begins to clump together to form cosmic structures, they get trapped in the matter and leave imprints as anisotropy in the CMB. Secondary anisotropy occurs after the cosmic background radiation has formed and already spread throughout the universe. This anisotropy is caused by the interaction of radiation with matter on cosmic scales, gravitational lensing effects resulting from the deflection of CMB light paths by dark matter (Aghanim, 2008; Bucher, 2015;

Chiba, 1997; Durrer, 1997; Gurzadyan and Kocharyan, 1993; Hu, 2006; Lukash, 1998; Smoot et al., 1977).

Polarization

Based on the measurements from COBE and WMAP, the CMB radiation exhibits an average temperature of 2,725 ± 0.001° K. Anisotropy leads to temperature variations in the CMB, with an amplitude of approximately ±0.0035° K. For instance, measurements conducted by COBE and WMAP (Hinshaw, 2006) successfully determined the orientation and amplitude of the dipole, as depicted in the figure 1 with an amplitude variation $\Delta T(\theta) = 3{,}358 \times 10^{-3} \cos\theta$ K.

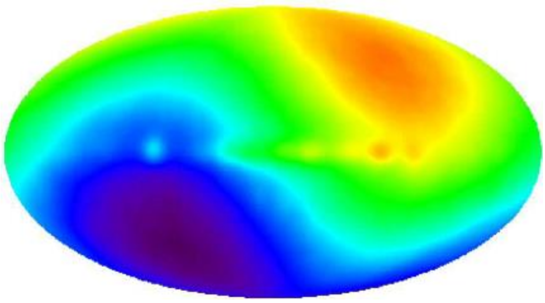

Figure 1. The CMB dipole observed by COBE and WMAP illustrates the distribution of temperature differences in CMB radiation, with the red zone indicating a warmer area and the blue zone representing a cooler area relative to the average temperature of 2,725 ±0,001° K (https://wmap.gsfc.nasa.gov/universe/bb_cosmo_fluct.html, 2014).

The polarization in Cosmic Microwave Background (CMB) radiation can be distinguished into two types, namely E-type polarization and B-type polarization. E-mode polarization in CMB occurs because CMB photons are polarized by the electric field formed by large-scale structures in the universe, such as galaxy clusters. In E-mode polarization, CMB photons are linearly polarized parallel or perpendicular to the direction of these large-scale structures. This happens due to the electromagnetic interaction between CMB photons and electrons in the electromagnetic field produced by these large structures. E-mode polarization exhibits a complex spiral pattern known as the E-mode. This spiral pattern emerges due to a phase shift between the horizontal and vertical polarizations of the CMB as it passes through large-scale structures in the universe. E-mode polarization provides crucial information about the distribution of matter in the universe, especially galaxy clusters, and enables researchers to measure cosmological parameters such as the density of matter and dark energy.

B-mode polarization in Cosmic Microwave Background (CMB) occurs because CMB photons are polarized by the magnetic field generated by small-scale structures in the universe, such as cosmic filaments or black holes. In B-mode polarization, CMB photons are circularly polarized either in the same direction or opposite direction to the magnetic field. This happens due to the electromagnetic interaction between CMB photons and the magnetic field produced by these small structures. B-mode polarization exhibits a rotating pattern known as the B-mode. Measuring B-mode polarization is challenging because it has a very small amplitude and is influenced by various factors such as gravitational lensing effects and instrumental noise. However, B-mode polarization can provide crucial information about the conditions of the universe during the cosmic inflation that occurred in the early stages of the universe's formation (Bucher, 2015).

Dipole, Quadrupole, and Octopole

The anisotropy in Cosmic Microwave Background (CMB) radiation is analyzed based on the concepts of dipole, quadrupole, octopole, and multipole, which divide the scale of temperature fluctuations in CMB radiation. The dipole represents the largest and most well-known temperature difference in CMB radiation, indicating the overall motion of the universe. The dipole takes the form of a divided sphere, with one side being warmer and the other colder. This temperature difference is measured at around 3 millikelvin. The quadrupole is a smaller but still significant temperature difference in CMB radiation compared to the dipole. The quadrupole takes the form of a divided sphere with four distinct parts. This temperature difference is measured at around 100 microkelvin. The octopole is an even smaller temperature difference in CMB radiation compared to the quadrupole. The octopole takes the form of a divided sphere with eight distinct parts. This temperature difference is measured at around 5 microkelvin (Bucher, 2015; Chiba, 1997; Hu, 2006; Smoot, 1977).

Multipole

The concept of multipole is a mathematical framework used to describe temperature variations in the Cosmic Microwave Background (CMB) radiation across different directions in the sky. In this concept, CMB radiation is decomposed into a series of components with progressively smaller temperature differences, referred to as multipole.

Mathematically, the decomposition of a function $\boldsymbol{f}(\theta,\varphi)$,representing the intensity or temperature of CMB radiation, is carried out using spherical harmonic functions $\boldsymbol{Y}_l^m(\theta,\varphi)$, and multipole coefficients $\boldsymbol{a}_{lm}$. The spherical harmonic function $\boldsymbol{Y}_l^m(\theta,\varphi)$ is a mathematical function that describes the variations in the temperature of CMB radiation across different directions in the sky. Meanwhile, the multipole coefficient $\boldsymbol{a}_{lm}$ is a mathematical quantity that represents the amplitude of the temperature difference in CMB radiation in each direction (Copi, 2005).

RESEARCH METHODS

The research method applied in this study is the literature review method (Zed, 2008). This study was conducted by elaborating on recent findings regarding Cosmic Microwave Background (CMB) radiation comprehensively. Data were obtained from intensity measurements of CMB radiation conducted by the COBE, WMAP, and Planck satellites. These data are presented in the form of temperature variables in spherical coordinates in FITS (Flexible Image Transport System) format files, which can be accessed through the official websites of COBE, WMAP, and Planck (Hanisch et al., 2001; Pence et al., 2010).

Next, a spherical harmonic transformation was applied to the FITS-formatted data. This transformation was carried out through several stages as follows:

- Defining a function representing the CMB temperature data,
- Solving the Laplace equation to obtain the expansion of this function,
- Obtaining the spherical harmonic coefficients $\boldsymbol{a}_{lm}$ as equations representing the dipole, quadrupole, octopole, and all multipole model configurations.

The obtained spherical harmonic coefficients are then used to derive the equation for the CMB radiation power spectrum, which provides a graphical representation of the entire CMB temperature distribution.

The final step involves analyzing the Earth's position's correlation with the CMB temperature distribution by elaborating on various anomalous patterns found in the dipole, quadrupole, and octopole models.

RESULTS AND DISCUSSION

Cosmic Microwave Background (CMB) radiation was initially discovered inadvertently in the form of excess noise while measuring sensitivity on a microwave antenna. The noise (CMB radiation) obtained resulted from spectrum analysis by comparing the reference signal and the output signal. However, following this discovery, CMB radiation became a dedicated research subject. Various astronomical missions, such as WMAP, COBE, and Planck, sent satellites equipped with sensitive microwave instruments and detectors. The intensity of CMB radiation is directly measured without involving noise measurements using reference signals.

The microwaves of CMB radiation represent an analog signal measured by instruments and detectors as fluctuations in voltage. The greater the radiation intensity, the larger the measured voltage, or in other words, the higher the temperature of the radiation. The relationship between intensity and temperature is governed by Planck's radiation law in Equation 2. Data from measurements of CMB radiation conducted by satellites such as WMAP, COBE, and Planck are commonly presented in the form of intensity or temperature. Published CMB radiation intensity or temperature data is typically presented in spherical coordinates, Mollweide projection maps, and Zenithal Equidistant Azimuthal (ZEA) projection maps (Bennet et al., 2013; Snyder, 1987; Snyder, 1989; Snyder and Voxland, 1989; Snyder, 1993), and is often published in the FITS (Flexible Image Transport System) format. FITS is a digital file format used for storing, transmitting, and manipulating scientific images and others, particularly in astronomy (Hanisch et al., 2001; Pence et al., 2010).

Laplace's Equation for $\boldsymbol{f}(r,\theta,\varphi)$

One way to analyze the distribution of a variable in a spatial domain is to transform it from the spatial domain to the frequency (spatial) domain, such as Fourier Transformation. Because the temperature data of CMB radiation is distributed on the surface of a sphere, the more appropriate transformation to use is the spherical harmonic transformation. Data from the CMB radiation temperature $\boldsymbol{T}(r,\theta,\varphi)$ can be represented in a function $\boldsymbol{f}(r,\theta,\varphi)$, This function needs to be expanded first to obtain the complete form of the spherical harmonic transformation equation that will be used.

The data from the CMB radiation temperature $\boldsymbol{T}(r,\theta,\varphi)$ represents temperature distribution data in the spatial domain and is entirely independent of time, indicating no temperature change over time ($\frac{dT}{dt}=0$) Therefore, the data satisfies the stationary condition. Hence, the expansion of the function $\boldsymbol{f}(r,\theta,\varphi)$ can be solved using Laplace's Equation:

$$\boldsymbol{\nabla}^2\boldsymbol{f}(r,\theta,\varphi)=0 \tag{3}$$

(Arfken, 2011; Boas, 2006) The complete form of the function is then obtained as:

$$\boldsymbol{f}(r,\theta,\varphi)=\boldsymbol{R}_l(r)\boldsymbol{Y}_l^m(\theta,\varphi)$$
$$=\left(Ar^l+\frac{B}{r^{l+1}}\right)(D\boldsymbol{P}_l^m(cos\theta))$$
$$\left(C_1e^{im\varphi}+C_2e^{-im\varphi}\right) \tag{4}$$

Since the CMB radiation temperature data $\boldsymbol{T}(r,\theta,\varphi)$ represents radiation intensity distribution data scattered on the surface of a sphere, the radial part of the spherical harmonic function used in this case is not dependent on the radial part (radial symmetry). In spatial analysis, it is crucial to perform orthonormalization to ensure that the harmonic functions for each combination of indices l and m are unique and possess essential properties for analysis. Therefore, it is necessary to perform orthogonality and normalization of $\boldsymbol{Y}_l^m(\theta,\varphi)$, giving:

$$\boldsymbol{Y}_l^m(\theta,\varphi) = \sqrt{\frac{2l+1}{2}\frac{(l-m)!}{(l+m)!}}\boldsymbol{P}_l^m(\cos\theta)\left(C_1 e^{im\varphi} + C_2 e^{-im\varphi}\right) \quad (5).$$

Spherical Harmonic Transformation (Multipole Coefficients and Power Spectrum)

From the obtained form of the spherical harmonic function, the temperature data of CMB radiation on the surface of the sphere can undergo spatial analysis using spherical harmonic transformation,

$$\boldsymbol{T}(\theta,\varphi) = \sum_{l=0}^{\infty}\sum_{m=-l}^{l}\boldsymbol{a}_{lm}\boldsymbol{Y}_l^m(\theta,\varphi), \quad (6)$$

where $\boldsymbol{a}_{lm}$ is the harmonic sphere coefficient or multipole coefficient representing each multipole model of the CMB radiation map. Subsequently, from the multipole coefficients $\boldsymbol{a}_{lm}$ equation for the CMB radiation power spectrum is obtained

$$C_l = \frac{1}{2l+1}\sum_{m=-l}^{l}|\boldsymbol{a}_{lm}|^2 \quad (7)$$

where, C_l represents the power spectrum of CMB radiation for each mode l. Through the CMB radiation power spectrum, we can analyze the overall fluctuations in the temperature distribution for each mode l based on the graph of the CMB radiation power spectrum.

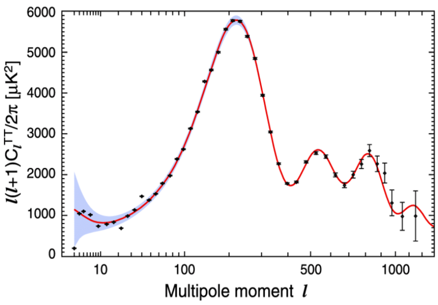

Figure 2. Graph of the CMB radiation Power Spectrum (Starkman, 2012).

Dipole Anomalies

The dipole is a model of anisotropic distribution on the CMB map generated from the analysis of temperature fluctuations in the anisotropy map of CMB with spherical harmonic coefficients, specifically for $l = 1$. In the dipole model, the temperature anisotropy on the CMB is distributed into two parts with a range of approximately 3 millikelvins. Thus, in the dipole anisotropy map, three distinct areas can be observed. The green region represents an area with an average temperature of 2,725° K. The red region corresponds to an area with a temperature approximately ±0.003° K higher than the average temperature of 2.725° K (warmer). On the other hand, the blue region represents an area with a temperature approximately ±0.003° K lower than the average temperature of 2,725° K (colder)

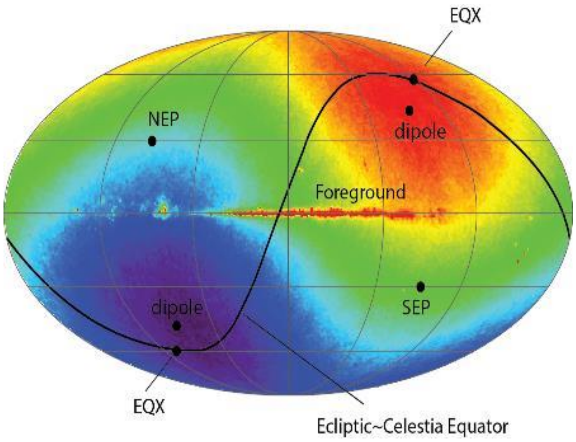

Figure 3. Dipole in barycentric coordinates with the reference plane of the galaxy (Copi, 2005; Tegmark, 2004).

From Figure 3, it is evident that the green-colored area forms a boundary plane separating the red and blue regions. This green area extends from the upper left to the lower right on the celestial sphere map, forming a sinusoidal pattern. The red and blue areas are positioned away from each other, with the lowest temperature concentration located in the bottom-left of the celestial sphere map, and the highest temperature concentration situated in the top-right. The highest and lowest positions of the dipole temperature amplitude are close to the two Earth equinox positions. The Earth equinox positions represent the nodes where the ecliptic plane and the celestial equator intersect. Therefore, drawing an imaginary line between these two dipole temperature amplitudes reveals an orientation parallel to both the ecliptic plane and the celestial equator (Aghanim et al., 2013; Copi, 2005; Gordon et al., 2005; Hinshaw, 2009; Schwarz, 2004), as depicted in Figure 4 below.

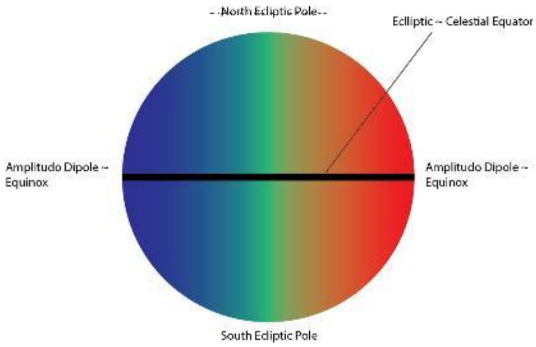

Figure 4. Dipole diagram with the ecliptic plane reference.

The boundary plane of the dipole, highlighted in green, appears distinctly perpendicular to the ecliptic plane, seemingly crossing both the northern and southern regions of the ecliptic plane (NEP and SEP). From Figure 4, it can be concluded that the pattern in the CMB anisotropy dipole is almost symmetric or quasi-symmetric. Considering that the presented CMB anisotropy map uses the galactic plane as a reference and is precisely centered on the equator of the map, with the position of the solar system, including Earth, relatively at the center of the map as the observer, it means that Earth is situated at the node intersection between the boundary plane of the dipole and the perpendicular ecliptic plane, right in between regions with contrasting temperatures. This situation should not occur, as it contradicts the isotropic nature of cosmology. In this dipole model, Earth's position is too significant for the observed polarization between the two regions. Therefore, it can be concluded that the dipole model of the CMB map indicates a lack of isotropy in the CMB map.

Quadrupole and Octopole Anomalies

The Quadrupole is a model of anisotropic distribution on the CMB map generated from the analysis of temperature fluctuations in the anisotropy map of CMB with spherical harmonic coefficients $l = 2$. In the quadrupole model, the temperature anisotropy on the CMB is distributed into four parts with a range of approximately 10 microkelvins, consisting of two cooler regions and two hotter regions.

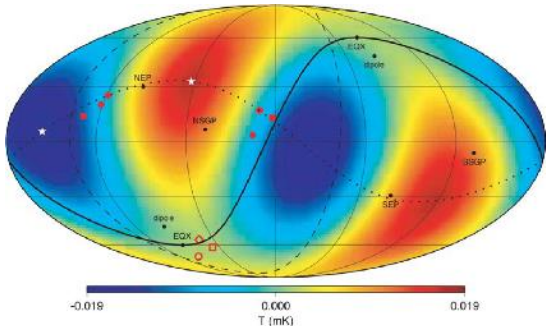

Figure 5. Quadrupole in barycentric coordinates with the galactic plane reference (Copi, 2005; Tegmark, 2004)

Figure 5 illustrates the quadrupole model on the CMB map presented in the sky map with the galactic plane as a reference. From the image, it is apparent that each formed area is bounded by a plane parallel to the meridian or longitude lines on the celestial sphere. Visibly, each region is arranged along the latitude lines on the celestial sphere, parallel to the galactic plane and foreground. Based on the amplitude of temperature anisotropy and the vector direction of each region, the quadrupole forms an imaginary plane (quadrupole plane) with a sinusoidal pattern along the latitude lines on the celestial sphere and nearly parallel to the galactic plane (Copi, 2005; Tegmark, 2003; Schwarz, 2004; Schwarz, 2016). This imaginary plane verifies that the visually observed pattern of the quadrupole plane is accurate. The ecliptic plane bisects the celestial sphere, and the quadrupole pattern divides into two regions, each with areas of hotter and colder temperatures. The imaginary ecliptic plane is perpendicular to the imaginary quadrupole plane because the sinusoidal pattern of the quadrupole plane extends across the northern and southern regions of the ecliptic plane (NEP and SEP) (Copi, 2005; Schwarz, 2004; Schwarz, 2016).

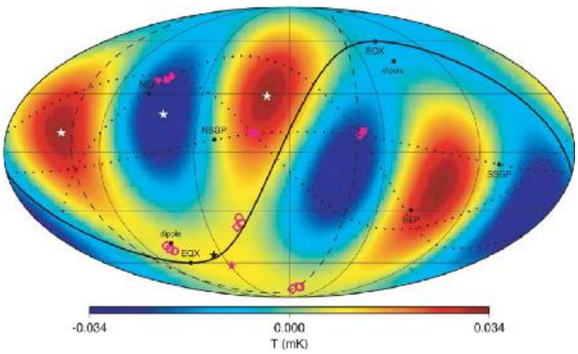

Figure 6. Octopole in barycentric coordinates with the galactic plane reference (Copi, 2005; Tegmark, 2004).

The Octopole is a model of anisotropic distribution on the CMB map generated from the analysis of temperature fluctuations in the anisotropy map of CMB with spherical harmonic coefficients $l = 3$. In the octopole model, the temperature anisotropy on the CMB is distributed into six parts with a range of approximately 5 microkelvins, consisting of three cooler regions and three hotter regions.

Figure 6 represents the octopole model on the CMB map presented in the sky map with the galactic plane as a reference. The octopole model forms more regions than the quadrupole model, but visually, the pattern formed by the octopole model bears many similarities to the quadrupole model. Similar to the quadrupole model, each region formed in the octopole model is parallel to the meridian or longitude lines on the celestial sphere. All regions are arranged along the latitude lines on the celestial sphere, parallel to the galactic plane and foreground (Copi, 2005; Schwarz, 2004; Schwarz, 2016). However, there are differences between the quadrupole and octopole models. Based on the amplitude of temperature anisotropy and the vector direction of each region, the octopole model forms three imaginary planes, two of which are almost parallel to the galactic plane and foreground. These three planes exhibit interesting characteristics and verify that the visually observed pattern of the octopole plane is accurate, with slight differences from the quadrupole plane.

The first imaginary plane of the octopole extends parallel to the galactic plane and foreground. The galactic plane is nearly perpendicular to the supergalactic plane, but this first imaginary plane of the octopole extends across the northern and southern regions of the supergalactic plane proportionally. This means that this plane is more proportionally perpendicular to the supergalactic plane than the galactic plane.

The second imaginary plane of the octopole is very similar to the quadrupole plane, almost parallel to the galactic plane, and extends with a sinusoidal pattern across the northern and southern regions of the ecliptic plane (NEP and SEP). Therefore, this octopole plane is perpendicular to the ecliptic plane.

The third imaginary plane of the octopole also extends from the northern and southern regions of the ecliptic plane (NEP and SEP). However, this plane is significantly distant from the celestial equator and is not parallel to the galactic plane. Despite extending from the northern and southern regions of the ecliptic plane (NEP and SEP) and being perpendicular to the ecliptic plane, this plane does not bisect the celestial sphere entirely. This is evident from the nodes of the imaginary lines of the two planes, which are located far from the center of the celestial sphere map.

Considering that the presented CMB anisotropy map uses the galactic plane as a reference and is precisely centered on the equator of the map, with the position of the solar system, including Earth, relatively at the center of the map as the observer, it means that Earth is situated at the intersection nodes among the 4 regions of the quadrupole with the ecliptic plane perpendicular to them and also at the intersection nodes among the 6 regions of the octopole with the ecliptic plane. This nearly symmetrical or quasi-symmetrical pattern with Earth at its center should not occur because it contradicts the isotropic nature of cosmology. Similar to the dipole model, Earth's position concerning the quadrupole and octopole models is too significant for the polarization occurring among the four quadrupole regions and the six octopole regions. Therefore, it can be concluded that the quadrupole and octopole models of the CMB map indicate that the CMB map is not isotropic.

CONCLUSION

From the analysis of the dipole, quadrupole, and octopole models, the quadrupole plane and the three octopole planes broadly exhibit similarities and interconnections. Furthermore, these imaginary planes indicate their unique positions as they are perpendicular to the ecliptic plane, which divides the quadrupole and octopole regions, resulting in nodes of intersection precisely at the center of the celestial sphere map. These nodes are similar to the nodes shown in the dipole model, albeit in a different manner. The dipole model illustrates a dipole plane parallel to the ecliptic plane intersecting with the plane that separates the hot and cold regions in the dipole model. This intersection forms a node at the center of the celestial sphere. The quasi-symmetric patterns and nodes of intersection generated at the center of the celestial sphere map seemingly suggest that the Earth, the solar system, and the Milky Way galaxy are not only the center of observation but also hold a special and significant position in the vast 93 billion light-year-sized celestial sphere. This situation should not occur because it strongly contradicts the isotropic principles of cosmology.

The concept of anisotropy itself, which underlies the study and analysis of models of anisotropic distributions of CMB radiation with spherical harmonic structure, already violates the isotropy principle. Even though temperature fluctuations in CMB anisotropy occur on a very small scale, statistically, these fluctuations remain highly significant in providing detailed information about the evolution and structure of the universe, and cannot be ignored. Therefore, it can be concluded that the three models of CMB radiation anisotropy indicate that the observer (in this case, Earth, the solar system, and the galaxy) holds a significant position in the universe, simultaneously proving the failure of the isotropy principle in cosmology. Hence, it is recommended to reconsider the isotropy principle in cosmology, at least for observable cosmic scales, as it has proven unsuccessful in its application.

REFERENCES

Abramo, L. R., and Pereira, T. S. (2010). Testing gaussianity, homogeneity, and isotropy with the cosmic microwave background. *Advances in Astronomy*, DOI: https://doi.org/10.1155/2010/378203

Aghanim, N., Armitage-Caplan, C., Arnaud, M., Ashdown, M., Atrio-Barandela, F., Aumont, J., ... & Rosset, C. (2014). Planck 2013 results. XXVII. Doppler boosting of the CMB: Eppur si muove. *Astronomy & Astrophysics*, *571*, A27. DOI: https://doi.org/10.48550/arXiv.1303.5087

Aghanim, N., Majumdar, S., and Silk, J. (2008). Secondary anisotropies of the CMB. *Reports on Progress in Physics*, 71(6), 066902. DOI: https://doi.org/10.1088/0034-4885/71/6/066902

Alpher, R. A., & Herman, R. (1948). Evolution of the Universe. *Nature*, 162(4124), 774-775. DOI: https://doi.org/10.1038/162774b0

Andrade, U., et al. (2018). A model-independent test of cosmic isotropy with low-z pantheon supernovae. *The Astrophysical Journal,* 865(2), 119. DOI: https://doi.org/10.3847/1538-4357/aadb90

Aprilia, R., Alifaturrohmah, M., Purnama, G., & Wahyuni, S. (2022). The Examination of the Wien's Displacement Constant with Simulation and Simple Numerical Approaches. *Physics Communication*, *6*(2), 71-78. DOI: https://doi.org/10.15294/physcomm.v6i2.39821

Arfken, G. B., Weber, H. J., and Harris, F. E. (2011). *Mathematical Methods for Physicists: A Comprehensive Guide*. Academic Press.

Assis, A. K., and Neves, M. C. (1995). History of the 2.7 K temperature prior to Penzias and Wilson. *Apeiron*, 2(3), 79-84.

Ball, D. W. (2013). Wien's displacement law as a function of frequency. *Journal of Chemical Education*, 90(9), 1250-1252. DOI: https://doi.org/10.1021/ed400113z

Bennett, C. L., et al. (2013). Nine-year Wilkinson Microwave Anisotropy Probe (WMAP) observations: Final maps and results. *The Astrophysical Journal Supplement Series*, 208(2), 20. DOI: https://doi.org/10.1088/0067-0049/208/2/20

Boas, M. L. (2006*). Mathematical methods in the physical sciences*. New Jersey : John Wiley & Sons.

Bucher, M. (2015). Physics of the cosmic microwave background anisotropy. *International Journal of Modern Physics D*, 24(02), 1530004. DOI: https://doi.org/10.1142/S0218271815300049.

Chiba, T., Mukohyama, S., and Nakamura, T. (1997). Anisotropy of the cosmic background radiation implies the violation of the strong energy condition in Bianchi type I universe. *Physics Letters B*, 408(1-4), 47-51. DOI: https://doi.org/10.1016/S0370-2693(97)00782-X.

Clarkson, C., and Maartens, R. (2010). Inhomogeneity and the foundations of concordance cosmology. *Classical and Quantum Gravity*, 27(12), 124008. DOI: https://doi.org/10.1088/0264-9381/27/12/124008.

Copi, C. J., Huterer, D., Schwarz, D. J., & Starkman, G. D. (2006). On the large-angle anomalies of the microwave sky. *Monthly Notices of the Royal Astronomical Society*, 367(1), 79-102. DOI: https://doi.org/10.1111/j.1365-2966.2005.09980.x.

Crawford, T. A. B., Hogg, D. C., and Hunt, L. E. (1961). A Horn-Reflector Antenna for Space Communication. *Bell System Technical Journal*, 40(4), 1095-1116. DOI: https://doi.org/10.1002/j.1538-7305.1961.tb01639.x.

Das, R. (2015). Wavelength-and frequency-dependent formulations of Wien's displacement law. *Journal of*

Chemical Education, 92(6), 1130-1134. DOI: https://doi.org/10.1021/acs.jchemed.5b00116.

Derlet, P. M., and Choy, T. C. (1996). Planck's radiation law: A many-body theory perspective. *Australian Journal of Physics*, 49(3), 589-606. DOI: https://doi.org/10.1071/PH960589.

Dicke, R. H., Peebles, P. J. E., Roll, P. G., & Wilkinson, D. T. (1965). Cosmic black-body radiation. *Astrophysical Journal*, 142, 414-419. DOI: https://doi.org/10.1086/148306.

Durrer, R. (1996). Anisotropies in the cosmic microwave background: Theoretical foundations. International *Journal of Theoretical Physics*, 36, 2469-2487. DOI: https://doi.org/10.1007/BF02768937.

Goodman, J. (1995). Geocentrism reexamined. Physical Review D, 52(4), 1821. DOI: https://doi.org/10.1103/PhysRevD.52.1821.

Gordon, C., Hu, W., Huterer, D., & Crawford, T. (2005). Spontaneous isotropy breaking: a mechanism for CMB multipole alignments. *Physical Review D*, 72(10), 103002. DOI: https://doi.org/10.1103/PhysRevD.72.103002.

Gurzadyan, V. G., and Kocharyan, A. A. (1993). A new view on the problem of anisotropy of the cosmic background radiation. *International Journal of Modern Physics D*, 2(01), 97-104. DOI: https://doi.org/10.1142/S0218271893000088.

Hanisch, R. J., Farris, A., Greisen, E. W., Pence, W. D., Schlesinger, B. M., Teuben, P. J., ... & Warnock, A. (2001). Definition of the flexible image transport system (FITS). *Astronomy and Astrophysics*, 376(1), 359-380. DOI: https://doi.org/10.1051/0004-6361:20010923.

Hinshaw, G., Nolta, M. R., Bennett, C. L., Bean, R., Doré, O., Greason, M. R., ... & Wright, E. L. (2007). Three-year Wilkinson Microwave Anisotropy Probe (WMAP) observations: Temperature analysis. *The Astrophysical Journal Supplement Series*, 170(2), 288. DOI: https://doi.org/10.1086/513698.

Hinshaw, G., Weiland, J. L., Hill, R. S., Odegard, N., Larson, D., Bennett, C. L., ... & Wright, E. L. (2009). Five-year Wilkinson Microwave Anisotropy Probe* observations: Data processing, sky maps, and basic results. *The Astrophysical Journal Supplement Series*, 180(2), 225. DOI: https://doi.org/10.1088/0067-0049/180/2/225.

Hu, W. (2006). Concepts in CMB anisotropy formation. In The Universe at High-z, Large-Scale Structure and the Cosmic Microwave Background (pp. 207-239). *Berlin, Heidelberg: Springer Berlin Heidelberg*. DOI: https://doi.org/10.1007/BFb0102588.

Land, K., and Magueijo, J. (2007). The axis of evil revisited. *Monthly Notices of the Royal Astronomical Society*, 378(1), 153-158. DOI: https://doi.org/10.1111/j.1365-2966.2007.11749.x.

Lukash, V. (1998, December 16-21). Anisotropy of CMB and Cosmological Model. In N. Dadhich & J. Narlikar (Eds.), Gravitation and Relativity: At the turn of the Millennium, 15th International Conference on General Relativity and Gravitation (p. 343). *Inter-University Centre for Astronomy and Astrophysics*. DOI: https://doi.org/10.48550/arXiv.astro-ph/9803212.

Narlikar, J. V., and Wickramasinghe, N. C. (1967). Microwave background in a steady-state universe. *Nature*, 216(5110), 43-44. DOI: https://doi.org/10.1038/216043a0.

Peebles, P. J. E. (1993). *Principles of Physical Cosmology* (Vol. 27). Princeton University Press.

Peebles, P. J. E., Schramm, D. N., Turner, E. L., & Kron, R. G. (1991). The case for the relativistic hot big bang cosmology. *Nature*, 352(6338), 769-776. DOI: https://doi.org/10.1038/352769a0.

Pence, W. D., Chiappetti, L., Page, C. G., Shaw, R. A., & Stobie, E. (2010). Definition of the flexible image transport system (FITS), version 3.0. *Astronomy and Astrophysics*, 524, A42. DOI: https://doi.org/10.1051/0004-6361/201015362.

Penzias, A.A. and Wilson, R.W. (1965) A Measurement of Excess Antenna Temperature at 4080 Mc/s. *The Astrophysical Journal*, 142, 419-421. DOI: https://doi.org/10.1086/148307.

Planck, M. (1900). The theory of heat radiation. *Entropie*, 144(190), 164.

Schwarz, D. J., Starkman, G. D., Huterer, D., & Copi, C. J. (2004). Is the low-ℓ microwave background cosmic? *Physical Review Letters*, 93(22), 221301. DOI: https://doi.org/10.1103/PhysRevLett.93.221301.

Schwarz, D. J., Copi, C. J., Huterer, D., & Starkman, G. D. (2016). CMB anomalies after Planck. *Classical and Quantum Gravity*, 33(18), 184001. DOI: https://doi.org/10.1088/0264-9381/33/18/184001.

Smoot, G. F., Gorenstein, M. V., and Muller, R. A. (1977). Detection of anisotropy in the cosmic blackbody radiation. *Physical Review Letters*, 39(14), 898. DOI: https://doi.org/10.1103/PhysRevLett.39.898.

Snyder, J. P. (1987). *Map Projections—A Working Manual (Vol. 1395).* US Government Printing Office.

Snyder, J. P. (1997). *Flattening the earth: two thousand years of map projections*. University of Chicago Press.

Snyder, J. P., and Steward, H. (Eds.). (1989). *Bibliography of Map Projections* (No. 1856). US Government Printing Office.

Snyder, J. P., and Voxland, P. M. (1989). *An Album of Map Projections* (No. 1453). US Government Printing Office.

Starkman, G.D., Copi, C.J., Huterer, D., & Schwarz, D.J. (2012). The Oddly Quiet Universe: How the CMB challenges cosmology's standard model. *Romanian Journal of Physics*, 57, 979-991. DOI: https://doi.org/10.48550/arXiv.1201.2459.

Tegmark, M., de Oliveira-Costa, A., and Hamilton, A. J. (2003). High resolution foreground cleaned CMB map from WMAP. *Physical Review D*, 68(12), 123523. DOI: https://doi.org/10.1103/PhysRevD.68.123523.

Weinberg, S. (2008). *Cosmology*. Oxford : Oxford University Press.

Williams, B. W. (2014). A Specific Mathematical Form for Wien’s Displacement Law as v max/T= constant. *Journal of Chemical Education*, 91(5), 623-623. DOI: https://doi.org/10.1021/ed400827f.

WMAP. (2014). *Fluctuations in the Cosmic Microwave Background*. Retrieved from https://wmap.gsfc.nasa.gov/universe/bb_cosmo_ fluct.html.

Zed, M. (2008). *Metode Penelitian Kepustakaan*. Yayasan Pustaka Obor Indonesia.

Zhou, Y., Zhao, Z.-C., and Chang, Z. (2017). Searching for a cosmological preferred direction with 147 rotationally supported galaxies. *The Astrophysical Journal*, 847(2), 86.